The concurrent record-breaking rainfall over Northwest India and North China in September 2021

Ying NA*[1], and Riyu LU[2,3]

[1]*Beijing Municipal Climate Center, Beijing* 100089*, China*

[2]*State Key Laboratory of Numerical Modeling for Atmospheric Sciences and Geophysical Fluid Dynamics, Institute of Atmospheric Physics, Chinese Academy of Sciences, Beijing* 100029, *China*

[3] *College of Earth and Planetary Sciences, University of the Chinese Academy of Sciences, Beijing* 100049*, China*

ABSTRACT

Extremely heavy rainfall occurred over both Northwest India and North China in September 2021. The precipitation anomalies were 4.1 and 6.2 times interannual standard deviation and broke the record since the observational data were available, i.e., 1901 and 1951, respectively. In this month, the Asian upper-tropospheric westerly jet extremely displaced poleward over West Asia, and correspondingly, an anomalous cyclone appeared over India. The anomalous cyclone transported abundant water vapor into Northwest India, leading to the heavy rainfall over there. In addition, the Silk Road pattern, a teleconnection pattern over the Eurasian continent and fueled by the heavy rainfall in Northwest India, contributed to the heavy rainfall in North China. Our study emphasizes the roles of atmospheric teleconnection patterns in concurrent rainfall extremes in the remote regions,

*Corresponding author: Ying NA
Email: naying@bj.cma.gov.cn

and the occurrence of rainfall extremes during the post- or pre-monsoon in the northern margins of monsoon regions.

Key words: extreme precipitation, Northwest India, North China, westerly jet, Silk Road pattern

Article Highlights:

- The record-breaking rainfall occurred over both Northwest India and North China in September 2021.
- The rainfall and large-scale circulations in this month resemble the peak rainy season (July and August), possibly due to warmer Eurasian continent.
- The Silk Road pattern is responsible for the concurrence of extremely heavy rainfall over the two remote regions.

https://doi.org/10.1007/s00376-022-2187-y

1. Introduction

In September 2021, extremely heavy rainfall occurred in both Northwest India and North China, triggering dire economic and societal consequences in these remote regions. According to India Meteorological Department, in 2021, 8 states and territories in Northwest India recorded excessive precipitation as compared to their respective September averages (https://weather.com/en-IN/india/monsoon/news/2021-10-01-india-ends-2021-monsoon-season-on-normal-note). Concurrent with the heavy rainfall in

Northwest India, precipitation over seven provinces in North China hit a record high since 1961 (Liu and Gao, 2021; Zhou et al., 2022b). Wei River, the tributary of Yellow River, with the peak flood in July and August normally, experienced the most severe autumn flood since 1935 (Li et al., 2022). Floods in four provinces affected more than 6 million people, led to 41 people killed or missing, destroyed farmland about 500 thousand hectares, and coasted economic losses totaled 15.34 billion yuan, according to the Chinese government (https://www.mem.gov.cn/xw/yjglbgzdt/202201/t20220123_407199.shtml).

The heavy rainfall in September 2021 is unexpected in the climatological sense, because the rainy season is prior to September over both Northwest India and North China. Influenced by the Asian summer monsoon, the rainy season is generally July and August over Northwest India and North China, corresponding to the march of Indian and East Asian summer monsoon, respectively, and subsequently in September, precipitation reduces remarkably (e.g., Krishnamurthy and Shukla, 2000; Wang and Lin, 2002).

The seasonal march of rainy season over both regions is closely connected to that of the upper-tropospheric Asian westerly jet (AWJ) (e.g., Liang and Wang, 1998; Ding and Chan, 2005; Chiang et al., 2017; Chowdary et al., 2019; Choudhury et al., 2021; Li et al., 2021). The AWJ is characterized by subseasonal meridional migration due to the seasonal change in warming and resultant meridional temperature gradient (Yeh et al., 1958; Kuang et al., 2007). When the AWJ reaches the northernmost position about 40°N in midsummer, precipitation over Northwest India and North China also reach the peak (e.g., Krishnamurthy and Shukla, 2000; Ding and Chan, 2005). In addition, the jet-rainfall relationship also exists on the interannual timescale: During the summer when AWJ is displaced poleward (equatorward), the rain bands tend to displaced poleward (equatorward), i.e., more (less) rainfall in Northwest India and North China (Liang and Wang, 1998; Lu, 2004; Wei et al., 2015; Du et al., 2016; Hong et al., 2021; Chowdary et al., 2022).

The summer precipitation variations over Northwest India and North China tend to be in phase (e.g., Kripalani and Singh, 1993; Wu, 2017; Wang et al., 2021). This in-phase relationship in summer rainfall can be well explained by the Rossby waves along the AWJ, known as the Silk Road pattern (SRP) (Lu et al., 2002; Wu and Wang, 2002; Saeed et al., 2011; Hong and Lu, 2016; Wu, 2017; Yadav, 2017). The SRP corresponds to anticyclonic (cyclonic) anomalies in the upper troposphere over West Asia and East Asia, respectively, enhancing (suppressing) the rainfall in Northwest India and North China. The Indian rainfall anomalies, affected by the SRP, can in turn trigger the downstream components of SRP, which propagates eastwards along the AWJ (Kripalani et al., 1997; Ding and Wang, 2005; Saeed et al., 2011; Greatbatch et al., 2013; Wei et al., 2013; Lin et al., 2017). The SRP can also contribute to the in-phase variations in precipitation between South Asia and East Asia (Wu, 2017; Liu and Huang, 2019). However, it should be mentioned that most of these previous studies focused on summer.

In the remnants of this paper, data and methods are presented in Section 2. The extreme rainfall in September 2021 broke the record over both Northwest India and North China is shown in Section 3. We illustrate the circulation anomalies responsible for the extreme rainfall and discuss the linkage of the extreme events between the two remote regions in Section 4. Summary is presented in Section 5.

2. Data and methods

The precipitation over India is from India Meteorological Department, with a 0.25°×0.25° resolution for 1901–2021 (Pai et al., 2014). The precipitation over China is from gauge-based observation of 2400 stations for 1951–2021 provided by the National Meteorological Information Center of China (http://101.200.76.197/en/?r=data/detail&dataCode=SURF_CLI_CHN_MUL_DAY_CES_V3.0). The precipitation anomaly over China in Figure 1a was calculated at each station respectively and then interpolated to 0.25°×0.25° grid by Cressman interpolation for plot. Wind, specific humidity, 2m air temperature, and vertical integral of water vapor flux are from ERA5 atmospheric reanalysis with a 0.25°×0.25° resolution for 1979–2021 (Hersbach et al., 2018). The climatological average and interannual standard deviation (STD) are derived by each variable from 1979 to 2020.

3. Extreme rainfall in September 2021

Figure 1a shows the precipitation anomalies for September 2021 in percentage. The percentage can highlight the anomalies compared with local climatological-mean precipitation, which exhibits a wide scope, ranging from tiny amount over the deserts over Northwest China to more than 400 mm over the western coastal of Indian subcontinent (Fig. 2b). Generally, rainfall was above normal in the northern parts of both India and China, and below normal in the southern parts. The extremely abnormal precipitation appeared over Northwest India and North China, where the precipitation in September 2021 was more than twice the climatological mean, with some areas even more than four times. The rain band appeared over Northwest India and North China in September 2021 (Fig. 2a), in a sharp contrast to normal years when the peak rainy season ended in both the regions and accordingly, the rainfall was decreased remarkably (Fig. 2b). Actually, the distribution of rainfall in September 2021 resembles somewhat that for climatological mean in July and August (Fig. 2c), which is the peak rainy season over Northwest India and North China, and thus the precipitation anomalies resemble the subseasonal differences between July/August and September (Fig. 2d).

We define Northwest India and North China as the areas where the percentage of precipitation anomalies in September 2021 was higher than 100% within (18°–30°N, 68°–80°E) and (33°–45°N, 105°–125°E), respectively, as shown by the white hatching in Figure 1a. The regional-mean precipitation in September 2021 was 308.1 and 226.2 mm for Northwest India and North China, respectively, and it broke the record in both the regions since the observational data are available, i.e., 1901 and 1951, respectively (Figs. 1b and 1c). The anomaly over Northwest India was 4.1 times STD, and the second largest dated back to more than 100 years ago (3.1 in 1917). In addition, the anomaly of precipitation over North China was 6.2 times STD, and this value was much greater than the second largest in 2011 (2.6).

The correlation coefficient between September precipitation over Northwest India and North China is 0.24 during 1951–2020, significant at the 0.05 confidence level, suggesting that the in-phase relationship in rainfall between Northwest India and North China exists in early autumn, in addition to summer. It should be mentioned that the region definitions for Northwest India and North China are based on the extreme rainfall occurred in September 2021, and thus may not be appropriate for accurately depict the statistical relationship in rainfall between these two regions during a long period. Therefore, the in-phase relationship would be underestimated by the correlation coefficient (0.24), which is calculated by the regional averages. Consider the active role of Indian rainfall, i.e., Indian rainfall affecting North China rainfall through the SRP, in the following we first discuss the causes of extreme precipitation over Northwest India in September 2021 and then turn to North China.

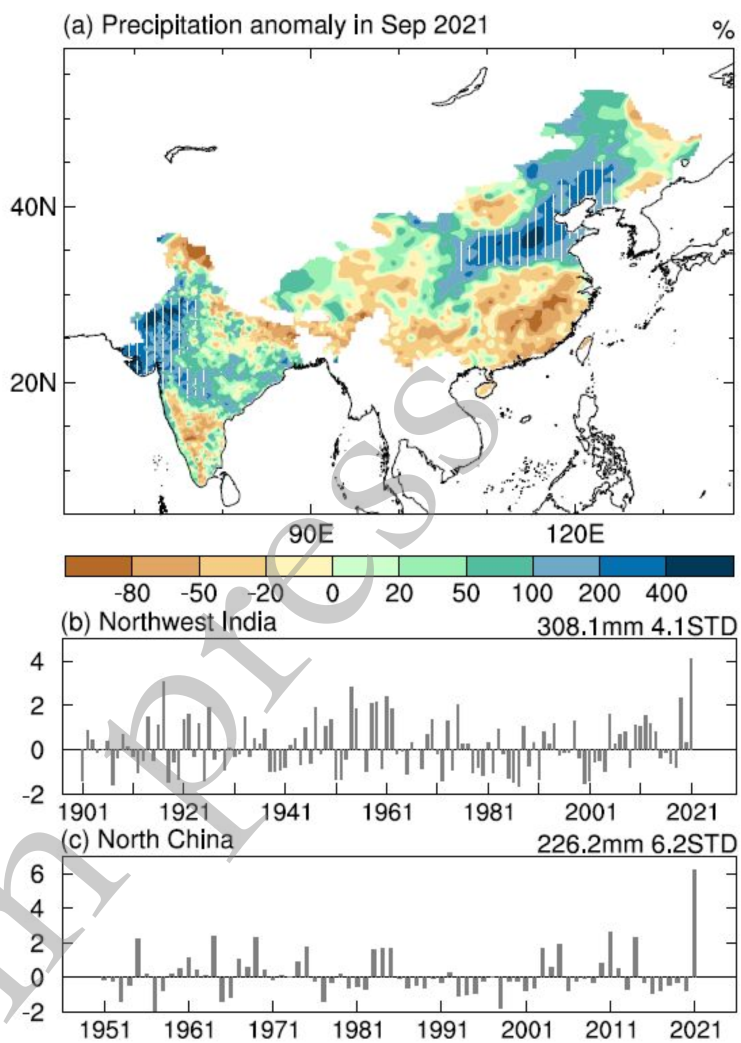

Fig. 1. (a) Percentage of precipitation anomalies (%) in September 2021 relative to climatology. Only the anomalies at the regions where climatological September precipitation is higher than 20 mm, except northwest China with sparse stations, are shown. The white hatching indicates Northwest India and North China. (b) Standardized precipitation averaged over Northwest India in September from 1901 to 2021. The numbers

in top right corner show the average precipitation and times of climatological STD in September 2021. (c) Same as (b), but for standardized precipitation averaged over North China.

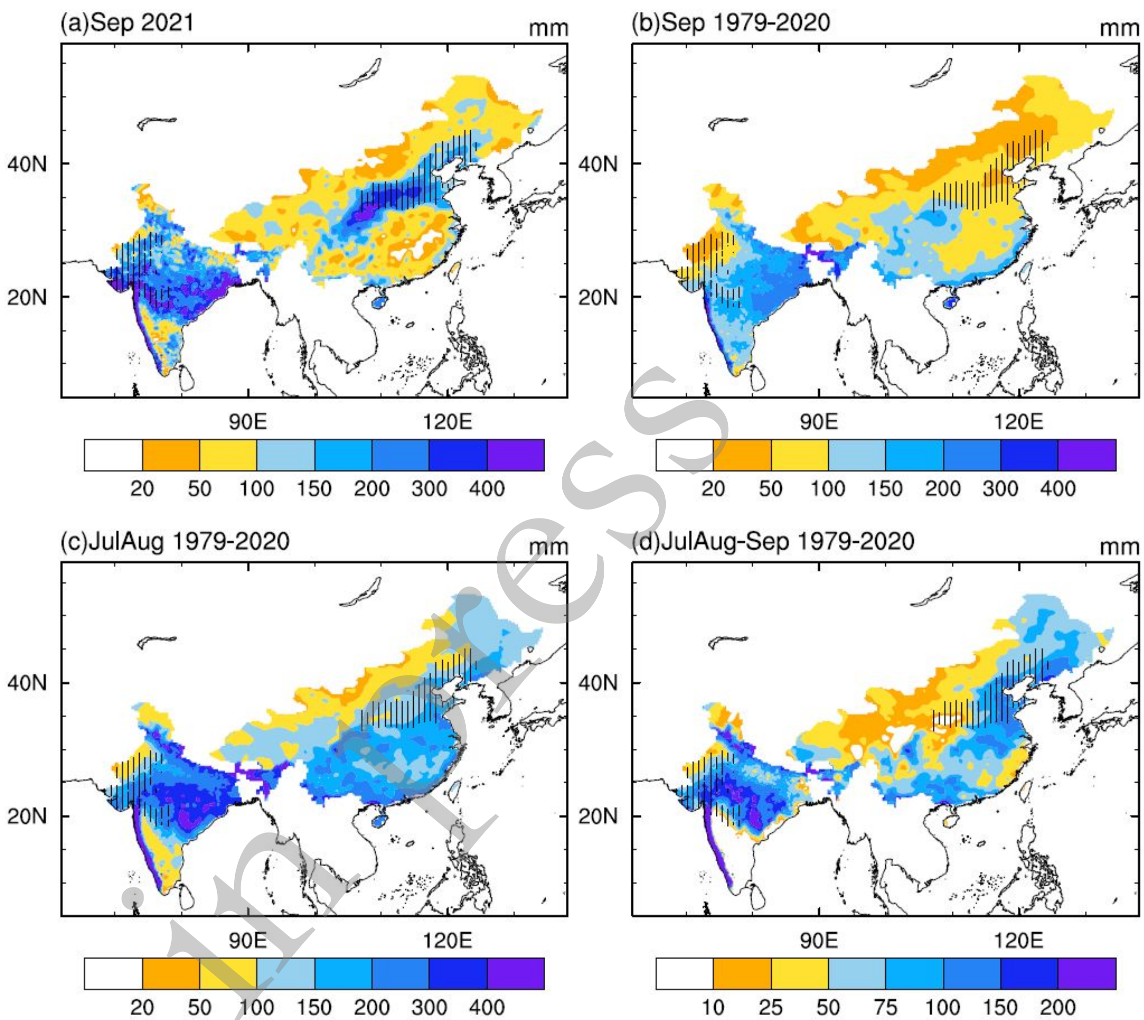

Fig. 2. Precipitation (mm) (a) in September 2021, (b) averaged in September during 1979–2020, (c) averaged in July and August during 1979–2020. (d) Difference between the precipitation averaged in July and August and precipitation in September during 1979–2020 (mm). Only the contours at the regions where climatological September precipitation is higher than 20 mm, except northwest China with sparse stations, are shown. The hatching indicates Northwest India and North China which is same as it in Figure 1.

4. Circulation anomalies

4.1 *For Northwest Indian rainfall*

The 200-hPa zonal wind anomalies in September 2021 are shown in Figure 3a. Westerly and easterly anomalies appeared to the north and south of AWJ axes, respectively. The zonal winds were extremely anomalous over West Asia, and the anomalies exceeded 2 times climatological STD at the majority of grids over this region. These zonal wind anomalies corresponded well to the poleward shift of AWJ. In particular, the jet axis (green bold dashed line) shifted poleward about 5 latitude degrees in September 2021 over West Asia in comparison with the climatology (black bold dashed line). Accordingly, the latitudes of the AWJ axis in September 2021 was comparable to, or even higher than, those for the climatology of July and August (Fig. 4b), when the AWJ usually reaches its northernmost location throughout the year, and the zonal wind anomalies in September 2021 were stronger than the subseasonal differences between July/August and September (Fig. 4a).

Considering the extreme zonal wind anomalies over West Asia, an index is specially defined as the difference between the zonal wind anomalies averaged over (40°–50°N, 50°–90°E) and (25°–35°N, 50°–90°E), to depict the AWJ variability over West Asia (hereafter abbreviated as WAWJ). A positive index represents the poleward displacement of WAWJ, and vice versa. The time series of standardized WAWJ index in September from 1979 to 2021 are shown in Figure 3b. The anomaly of WAWJ index in 2021 was 2.7 times climatological STD and was the largest since 1979.

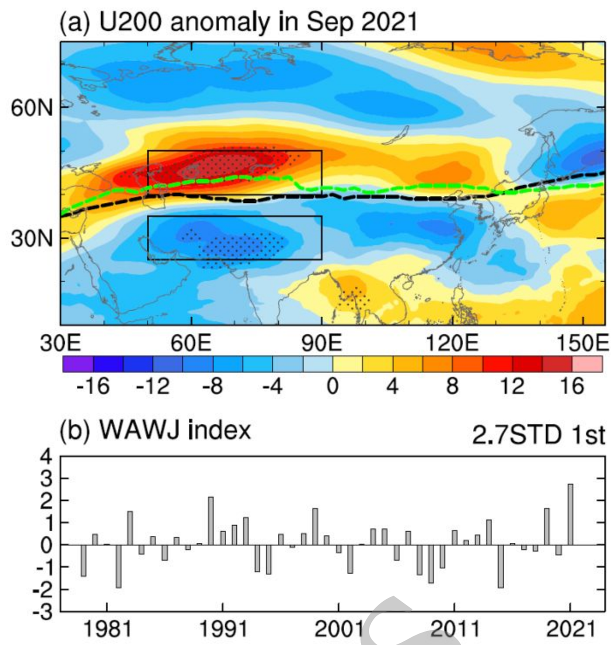

Fig. 3. (a) Anomalies of 200-hPa zonal wind (m s^{-1}) in September 2021. Dots indicate the anomalies exceeding ±2 times STD. Green and black dash lines show the AWJ axis in September 2021 and the climatological AWJ axis, respectively. The black boxes indicate the regions (25°–35°N, 50°–90°E) and (40°–50°N, 50°–90°E) used to define WAWJ index. (b) Standardized WAWJ index in September from 1979 to 2021. The numbers in right corner show the anomalous times of STD in September 2021 and the rank of it since 1979.

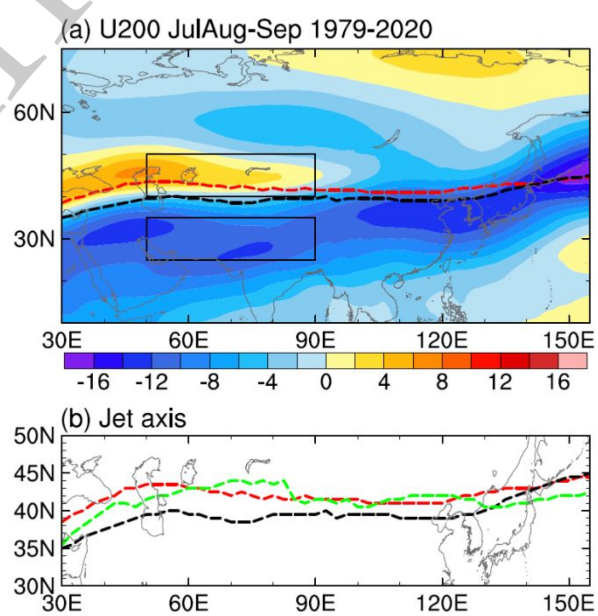

Fig. 4. (a) Difference of 200-hPa zonal wind (m s^{-1}) between the average of July and August and it in September during 1979–2020. (b) Green, black, and red dash lines show the AWJ axis in September 2021, the climatological AWJ axis in September, and the climatological AWJ axis averaged in July and August, respectively.

The lower-tropospheric winds and resultant water vapor flux are crucial for inducing precipitation, and anomalous winds and water vapor flux at 850 hPa (Fig. 5) do explain well the precipitation enhancement in September 2021. There were significant cyclonic anomalies over India and the cyclonic wind anomalies were generally over two times the climatological STD (Fig. 5a). These anomalous winds associated with Indian cyclone transported abundant water vapor at Northwest India (Fig. 5b), consistent with the vertically integrated water vapor flux (Fig. 6), confirming the crucial role of lower-tropospheric winds in transporting total water vapor. It should be mentioned that the monthly circulation anomalies are the sum of various synoptic disturbances including the Cyclone Gulab. This cyclone, which initiated over the Bay of Bengal on September 24 and passed through India afterwards, greatly contributed to the precipitation enhancement over Northwest India (figures not shown).

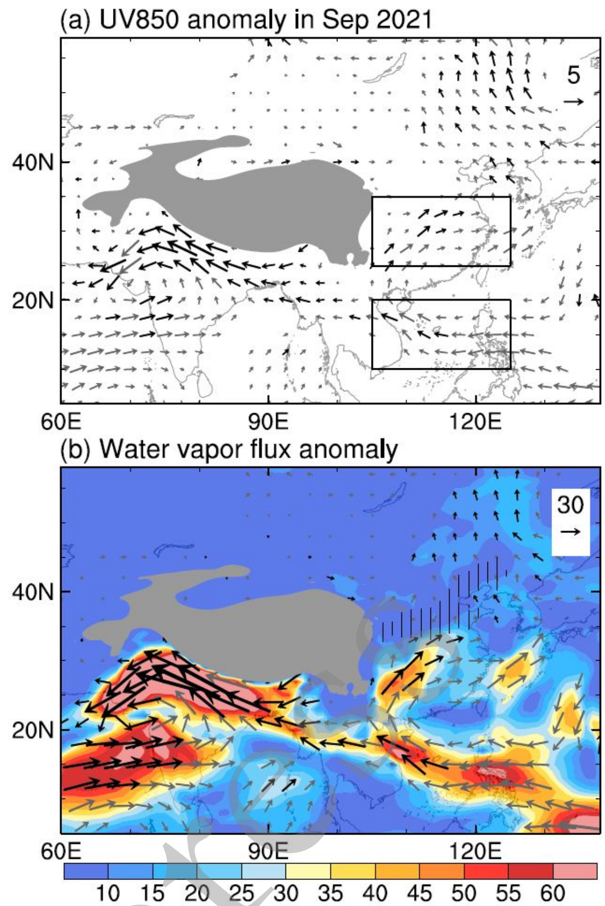

Fig. 5. (a) Anomalies of 850-hPa wind (m s^{-1}) in September 2021. Black and grey vectors show the wind anomalies exceeding ±2 and ±1 times climatological STD, respectively. The black boxes indicate the regions (25°–35°N, 105°–125°E) and (10°–20°N, 105°–125°E) used to define anticyclone index in Section 4.2. (b) Anomalies of water vapor flux (m s^{-1} g kg^{-1}) at 850 hPa in September 2021. The contours show the value and the vectors show the anomalies exceeding ±2 (black) and ±1 (grey) times STD. The black hatching indicates North China which is same as it in Figure 1. The grey shading shows the 2000 m topography.

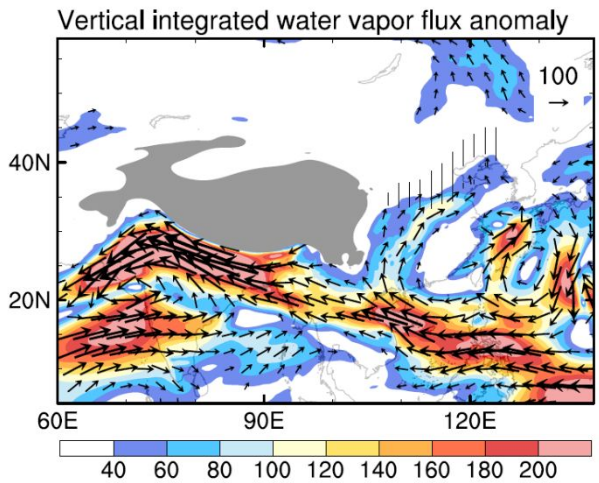

Fig. 6. Anomalies of vertical integrated water vapor flux from the surface to 100 hPa (kg m^{-1} s^{-1}) in September 2021. Only the values greater than 40 kg m^{-1} s^{-1} are shown. The black hatching indicates North China which is same as it in Figure 1. The grey shading shows the 2000 m topography.

The concurrent WAWJ poleward displacement in the upper troposphere and Indian cyclonic anomalies in the lower troposphere may not be accidental. Figure 7 shows the 850-hPa horizontal wind regressed onto the WAWJ index during 1979–2020. There are significant cyclone anomalies at 850 hPa over India in association with the poleward displacement of WAWJ, suggesting the close relationship between these circulation anomalies in the upper and lower troposphere.

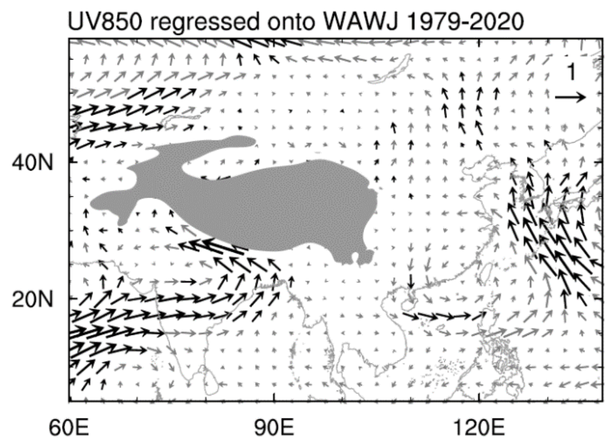

Fig. 7. 850-hPa horizontal wind (m s^{-1}) regressed onto the WAWJ index during 1979–2020. The black vectors show the wind anomalies significant at the 0.05 level, according to Student's test. The grey shading shows the 2000 m topography.

A question arises: What is the reason for the poleward displacement of WAWJ in September 2021? Considering that the meridional temperature gradient plays a crucial role in determining the meridional migration of AWJ, the surface air temperature anomalies in September 2021 are shown in Figure 8. The temperature anomalies were extremely positive over West Asia, exceeding 2 times the climatological STD. On the other hand, the temperatures were below normal to the north of about 40°N in the Eurasian continent, and the temperature anomalies were generally weak in the Indian Ocean. As a result, the meridional temperature gradient was strengthened over the mid-high latitudes and weakened over the low latitudes in West Asia, corresponding to the poleward displaced WAWJ. The anomaly of temperature averaged over West Asia (25°–40°N, 50°–90°E) in September 2021 was the largest since 1979 (Fig. 8b), and the correlation coefficient between the temperature averaged over this region and the WAWJ index is 0.41 during 1979–2020, significant at the 0.01 confidence level. Thus, the extreme temperature anomalies over West Asia in September 2021 may contribute to the poleward displacement of WAWJ.

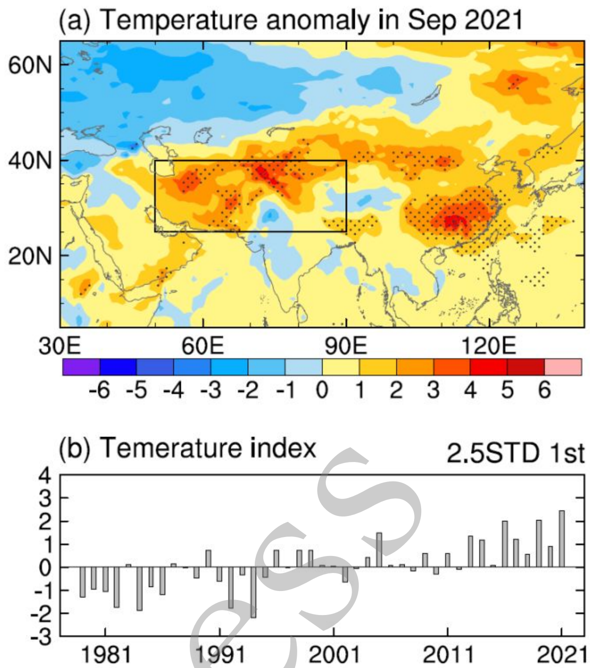

Fig. 8. (a) Surface temperature anomalies in September 2021 (°C). Dots indicate the anomalies exceeding ±2 times STD. Black boxes show the region (25°–40°N, 50°–90°E) used for define temperature index. (b) Time series of standardized September temperature anomalies averaged over the region shown in (a) from 1979 to 2021. The numbers in right corner show the anomalous times of STD in September 2021 and the rank of it since 1979.

4.2 *For North China*

Over East Asia, in September 2021 there were also westerly anomalies to the north of jet axis and easterly anomalies to the south, corresponding to the poleward displacement of jet axis (Fig. 3a), although these anomalies were not so extreme as those over West Asia. The latitude of the jet axis in September 2021 was also comparable to, or even higher than, the climatological location of July–August jet axis (Fig. 4b). As mentioned in the introduction, the poleward shifted jet would favor the heavier rainfall in North China.

The lower-tropospheric circulation anomalies were in favor of water vapor transportation into North China in September 2021 (Fig. 5). Extremely anomalous southwesterlies in association with the anticyclonic anomaly over South China and the western North Pacific transported more water vapor into the western part of North China, and the southerly or southeasterly anomalies over the Yellow Sea and coastal regions of China favored more water vapor transportation into the eastern part of North China. The combination of the anomalous southwesterlies and southeasterlies induced the extreme precipitation over North China. It should be mentioned that the southerly/southeasterly anomalies, albeit much weaker than the southwesterly anomalies, were crucial for water vapor convergence over North China (Figs. 5b and 6), due to the sharp south-to-north decrease of specific humidity over eastern China in September.

The southerly and southeasterly anomalies at 850 hPa over the coastal regions of China and Yellow Sea correspond to southerly anomalies in the upper troposphere. In September 2021 there were southerly anomalies at 200 hPa over eastern China, and there were also strong southerly and northerly anomalies over the midlatitude Eurasian continent and Japan (Fig. 9a). These meridional wind anomalies resembled well the SRP, and the SRP in September 2021 was extremely anomalous and broke the record (Fig. 9b). Here, the SRP index is defined as the algebraic sum of 200-hPa meridional wind anomalies at the four centers along 40°N as marked in Figure 9a, i.e., V200(50°E) -V200(80°E) +V200(110°E) -V200(140°E).

The concurrence between the SRP and lower-tropospheric southerly/southeasterly anomalies over the coastal regions of China and Yellow Sea is not limited to the specific case of September 2021, but also exists in normal years. Figure 10 shows the 850-hPa horizontal wind (m s^{-1}) regressed onto the SRP index during 1979–2020. Stronger SRP corresponds to significant southeasterly anomalies over the Yellow Sea and northern part of East China, which leads to the wind convergence over North China. Therefore, the extremely anomalous SRP in September 2021 was associated with anomalous lower-tropospheric southeasterlies and wind convergence over North China.

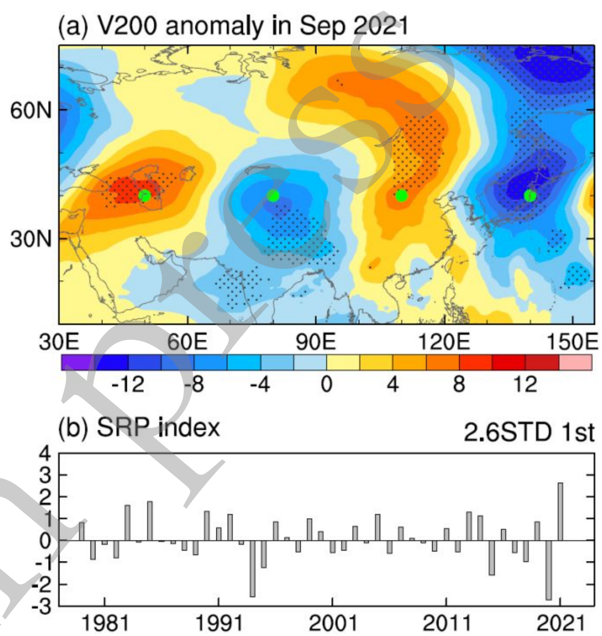

Fig. 9. (a) Anomalies of 200-hPa meridional wind (m s^{-1}) in September 2021. Dots indicate the anomalies exceeding ±2 times STD. Green dots indicate the points (40°N, 50°E), (40°N, 80°E), (40°N, 110°E), and (40°N,140°E) used to define SRP index. (b) Standardized SRP index in September from 1979 to 2021. The numbers in right corner show the anomalous times of STD in September 2021 and the rank of it since 1979.

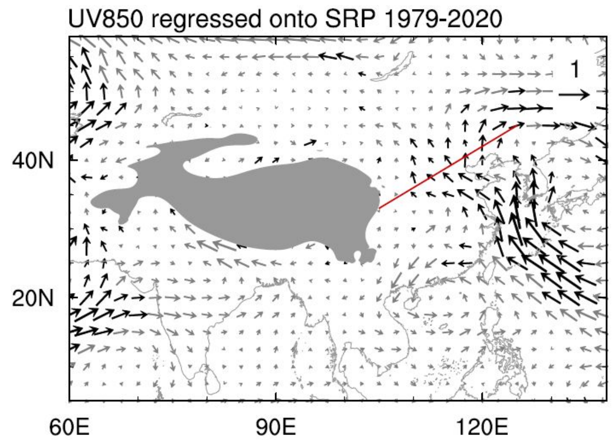

Fig. 10. 850-hPa horizontal wind (m s^{-1}) regressed onto the SRP index (SRPI) during 1979–2020. The black vectors show the wind anomalies significant at the 0.05 level, according to Student's test. The grey shading shows the 2000 m topography. The red line (from 33°N, 105°E to 45°N, 125°E) illustrates the rainfall enhancement over North China in September 2021.

The SRP is crucial for the linkage between circulation and precipitation anomalies over West and East Asia. Hong et al. (2021) stated that the poleward displacement of WAWJ is associated with the enhanced SRP, and the SRP can be significantly fueled by the precipitation over Northwest India through latent heat release (Ding and Wang, 2005). Our results show the SRP can lead to the enhanced precipitation over North China. As a result, the SRP is responsible for the concurrence of extremely heavy rainfall over the two remote regions in September 2021.

On the other hand, the anomalous anticyclone over South China and the western North Pacific in September 2021 might be an independent factor. As shown in Fig. 5, the southwesterly anomalies associated with the anticyclonic anomaly transported more water vapor northward from ocean in this month. During 1979–2020, it shows weak or even contrast relationships to the WAWJ displacement (Fig. 7), SRP (Fig. 10), and lower-tropospheric cyclonic anomaly over India (Fig. 11). Therefore, we can conclude that both this anomalous anticyclone and the SRP contributed to the extremely heavy rainfall in North China in September 2021.

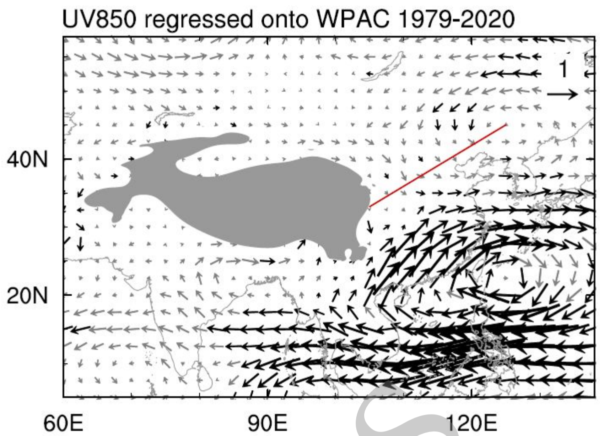

Fig. 11. 850-hPa horizontal wind (m s^{-1}) regressed onto the index of anomalous anticyclone over west Pacific (WPAC) during 1979–2020. Here, the index is defined as the difference between the 850-hPa zonal wind anomalies averaged over (25°–35°N, 105°–125°E) and (10°–20°N, 105°–125°E), where the winds were extremely anomalous in September 2021 as shown in Figure 5a. The black vectors show the wind anomalies significant at the 0.05 level, according to Student's test. The grey shading shows the 2000 m topography. The red line (from 33°N, 105°E to 45°N, 125°E) illustrates the rainfall enhancement over North China in September 2021.

Recently, Liu et al. (2022) investigated the effects of tropical SST anomalies on the extreme rainfall event over North China in September 2021. They suggested that the SST anomalies in the tropical Indian Ocean, Pacific and Atlantic strengthened the convection over the Maritime Continent and northern Indian Peninsula which contributed to the anticyclonic anomaly over the western North Pacific and resulted extreme rainfall over North China. This study, however, emphasizes the role of internal atmospheric variability, i.e., the midlatitude atmospheric circulations, including the SRP and related lower-tropospheric southerlies or southeasterlies.

5. Summary

Record-breaking precipitation occurred simultaneously over Northwest India and North China in September 2021. The precipitation extremes over Northwest India was contributed by the extremely poleward displaced WAWJ and corresponding water vapor transported by the anomalous Indian cyclone. The WAWJ displaced to the northernmost position which might be contributed by the extremely warm temperature over West Asia and resultant meridional temperature gradient. Furthermore, the SRP was extremely anomalous in the month, possibly induced by the Indian rainfall anomalies. The anomalous SRP favored the extreme rainfall in North China through the poleward displaced upper-tropospheric westerly jet over East Asia and the lower-tropospheric southeasterly anomalies, in combination with the water vapor transported by the anomalous anticyclone over the western North Pacific.

The present study indicated that the precipitation and circulation in September 2021 resemble those in the peak rainy season, i.e., July and August. This may be contributed by the extremely warm temperatures in the Eurasian continent, which could induce the poleward displacement of upper-tropospheric westerly jet (e.g., Lu et al., 2007; Seidel et al., 2008; Pena-Ortiz et al., 2013; Simpson et al., 2014). Such a poleward displacement would be more remarkable during the seasonal transitions, when the surface temperatures experience rapid changes and thus the jet location is more sensitive to the temperature changes (Voigt and Shaw, 2016; Chen et al., 2020). Therefore, climate extremes during the seasonal transitions should be emphasized, in addition to the extremes during the peak warm or cold seasons that are currently under wide studies (Endo et al., 2021; Yang et al., 2021; Zhou et al., 2022a). On the other hand, the present results suggest that climate extremes in one region can be related to, or lead to, those in other regions, through the atmospheric teleconnection patterns. It is widely believed that the climate extremes would occur more frequently and their intensities would be enhanced under the global warming. Therefore, the more frequent and stronger climate extremes would trigger the atmospheric teleconnections more frequently, which in turn induce the climate extremes in remote regions worldwide (Lau and Kim, 2012; Orsolini et al., 2015; Boers et al., 2019).

Acknowledgments. The authors greatly appreciate the comments and suggestions from the two anonymous reviewers. This study was supported by the National Natural Science Foundation of China (Grant NO. 42105064), the Second Tibetan Plateau Scientific Expedition and Research (STEP) program (Grant NO. 2019QZKK0102) and China Meteorological Administration program (Grant NO. CXFZ2021J030).

Data Availability Statements. The gauge-based precipitation dataset over China can be accessed at http://101.200.76.197/en/?r=data/detail&dataCode=SURF_CLI_CHN_MUL_DAY_CES_V3.0. The precipitation dataset over India can be accessed at https://www.imdpune.gov.in/Clim_Pred_LRF_New/Grided_Data_Download.html. ERA5 atmospheric reanalysis can be accessed at https://cds.climate.copernicus.eu/cdsapp#!/dataset/reanalysis-era5-pressure-levels?tab=overview.

REFERENCES

Boers, N., B. Goswami, A. Rheinwalt, B. Bookhagen, B. Hoskins, and J. Kurths, 2019: Complex networks reveal global pattern of extreme-rainfall teleconnections. *Nature*, **566**, 373-377.

Chen, G., P. Zhang, and J. Lu, 2020: Sensitivity of the latitude of the westerly jet stream to climate forcing. *Geophysical Research Letters*, **47**, e2019GL086563.

Choudhury, D., D. Nath, and W. Chen, 2021: The modulation of Indian summer monsoon onset processes during ENSO through equatorward migration of the subtropical jet stream. *Climate Dynamics*, **57**, 141-152.

Chowdary, J. S., K. Hu, G. Srinivas, Y. Kosaka, L. Wang, and K. K. Rao, 2019: The Eurasian jet streams as conduits for East Asian monsoon variability. Current Climate Change Reports, **5**, 233-244.

Chowdary, J. S., A. S. Vibhute, P. Darshana, A. Parekh, C. Gnanaseelan, and R. Attada, 2022: Meridional displacement of the Asian jet and its impact on Indian summer monsoon rainfall in observations and CFSv2 hindcast. *Climate Dynamics*, **58**, 811-829.

Ding, Q., and B. Wang, 2005: Circumglobal teleconnection in the northern hemisphere summer. *Journal of Climate*, **18**, 3483-3505.

Ding, Y., and J. Chan, 2005: The East Asian summer monsoon: An overview. *Meteorology and Atmospheric Physics*, **89**, 117-142.

Du, Y., T. Li, Z. Xie, and Z. Zhu, 2016: Interannual variability of the Asian subtropical westerly jet in boreal summer and associated with circulation and SST anomalies. *Climate Dynamics*, **46**, 2673-2688.

Endo, H., A. Kitoh, R. Mizuta, and T. Ose, 2021: Different future changes between early and late summer monsoon precipitation in East Asia. *Journal of the Meteorological Society of Japan*, **99**, 1501-1524.

Greatbatch, R. J., X. Sun, and X.-Q. Yang, 2013: Impact of variability in the Indian summer monsoon on the East Asian summer monsoon. *Atmospheric Science Letters*, **14**, 14-19.

Hong, X., R. Lu, and S. Li, 2021: Interannual relationship between the West Asian and East Asian jet meridional displacements in summer. *Journal of Climate*, **34**, 621-633.

Kripalani, R. H., and S. V. Singh, 1993: Large scale aspects of India-China summer monsoon rainfall. *Advances in Atmospheric Sciences*, **10**, 71-84.

Krishnamurthy, V., and J. Shukla, 2000: Intraseasonal and interannual variability of rainfall over India. *Journal of Climate*, **13**, 4366-4377.

Kuang, X., Y. Zhang, and J. Liu, 2007: Seasonal variations of the East Asian subtropical westerly jet and the thermal mechanism. *Journal of Meteorological Research*, **21**, 192-203.

Hersbach, H., B. Bell, P. Berrisford, G. Biavati, A. Horányi, J. Muñoz Sabater, J. Nicolas, C. Peubey, R. Radu, I. Rozum, D. Schepers, A. Simmons, C. Soci, D. Dee, J. Thépaut, 2018: ERA5 hourly data on pressure levels from 1979 to present. Copernicus Climate Change Service (C3S) Climate Data Store (CDS). (Accessed on <01-11-2021 >), 10.24381/cds.bd0915c6.

Lau, W. K. M., and K.-M. Kim, 2012: The 2010 Pakistan flood and Russian heat wave: Teleconnection of hydrometeorological extremes. *Journal of Hydrometeorology*, **13**, 392-403.

Li, J., B. Liu, and J. Mao, 2021: Climatological intraseasonal oscillation in the middle–upper troposphere and its effect on the northward migration of the East Asian westerly jet and rain belt over eastern China. *International Journal of Climatology*, **41**, 5084-5099.

Li, W., and Coauthors, 2022: State of China's climate in 2021. *Atmospheric and Oceanic Science Letters*, 100211.

Liang, X.-Z., and W.-C. Wang, 1998: Associations between China monsoon rainfall and tropospheric jets. *Quarterly Journal of the Royal Meteorological Society*, **124**, 2597-2623.

Lin, Z., R. Lu, and R. Wu, 2017: Weakened impact of the Indian early summer monsoon on North China rainfall around the late 1970s: Role of basic-state change. *Journal of Climate*, **30**, 7991-8005.

Liu, B., C. Zhu, S. Ma, and Y. Yan, 2022: Combined effects of tropical Indo-Pacific-Atlantic SST anomalies on record-breaking floods over Central-North China in September 2021. *Journal of Climate*, in press. https://doi.org/10.1175/JCLI-D-21-0988.1.

Liu, L., and S. Gao, 2021: Analysis of the September 2021 atmospheric circulation and weather. *Meteorological Monthly*, **47**, 1555-1560. (in Chinese)

Liu, Y., and R. Huang, 2019: Linkages between the South and East Asian monsoon water vapor transport during boreal summer. *Journal of Climate*, **32**, 4509-4524.

Lu, R., 2004: Associations among the components of the East Asian summer monsoon system in the meridional direction. *Journal of the Meteorological Society of Japan. Ser. II*, **82**, 155-165.

Lu, R.-Y., J.-H. Oh, and B.-J. Kim, 2002: A teleconnection pattern in upper-level meridional wind over the North African and Eurasian continent in summer. *Tellus A: Dynamic Meteorology and Oceanography*, **54**, 44-55.

Lu, J., G. A. Vecchi, and T. Reichler, 2007: Expansion of the Hadley cell under global warming. *Geophysical Research Letters*, **34**, L06805.

Orsolini, Y. J., L. Zhang, D. Peters, K. Fraedrich, X. Zhu, A. Schneidereit, and B. Hurk, 2015: Extreme precipitation events over North China in August 2010 and their link to eastward-propagating wave-trains across Eurasia: observations and monthly forecasting. *Quarterly Journal of the Royal Meteorological Society*, **141**, 3097-3105.

Pai, D. S., L. Sridhar, M. Rajeevan, O. P. Sreejith, N. S. Satbhai, and B. Mukhopadhyay, 2014: Development of a new high spatial resolution (0.25 degrees × 0.25 degrees) long period (1901-2010) daily gridded rainfall data set over India and its comparison with existing data sets over the region. *Mausam*, **65**, 1–18.

Pena-Ortiz, C., D. Gallego, P. Ribera, P. Ordonez, and M. D. C. Alvarez-Castro, 2013: Observed trends in the global jet stream characteristics during the second half of the 20th century. *Journal of Geophysical Research: Atmospheres*, **118**, 2702-2713.

Saeed, S., W. A. Müller, S. Hagemann, D. Jacob, M. Mujumdar, and R. Krishnan, 2011: Precipitation variability over the South Asian monsoon heat low and associated teleconnections. *Geophysical Research Letters*, **38**, L08702.

Seidel, D. J., Q. Fu, W. J. Randel, and T. J. Reichler, 2008: Widening of the tropical belt in a changing climate. *Nature Geoscience*, **1**, 21-24.

Simpson, I. R., T. A. Shaw, and R. Seager, 2014: A diagnosis of the seasonally and longitudinally varying midlatitude circulation response to global warming. *Journal of the Atmospheric Sciences*, **71**, 2489-2515.

Voigt, A., and T. A. Shaw, 2016: Impact of regional atmospheric cloud radiative changes on shifts of the extratropical jet stream in response to global warming. *Journal of Climate*, **29**, 8399-8421.

Wang, B., and H. Lin, 2002: Rainy season of the Asian–Pacific summer monsoon. *Journal of Climate*, **15**, 386-398.

Wang, L., P. Xu, and J. S. Chowdary, 2021: Chapter 14—Teleconnection along the Asian jet stream and its association with the Asian summer monsoon. In J. Chowdary, A. Parekh, & C. Gnanaseelan (Eds.), Indian Summer Monsoon Variability (pp. 287–298). Elsevier.

Wei, W., R. Zhang, M. Wen, X. Rong, and T. Li, 2013: Impact of Indian summer monsoon on the South Asian High and its influence on summer rainfall over China. *Climate Dynamics*, **43**, 1257-1269.

Wei, W., R. Zhang, M. Wen, B.-J. Kim, and J.-C. Nam, 2015: Interannual variation of the South Asian high and its relation with Indian and East Asian summer monsoon rainfall. *Journal of Climate*, **28**, 2623-2634.

Wu, R., 2017: Relationship between Indian and East Asian summer rainfall variations. *Advances in Atmospheric Sciences*, **34**, 4-15.

Wu, R., and B. Wang, 2002: A contrast of the East Asian summer monsoon–ENSO relationship between 1962–77 and 1978–93. *Journal of Climate*, **15**, 3266-3279.

Yadav, R. K., 2017: Midlatitude Rossby wave modulation of the Indian summer monsoon. *Quarterly Journal of the Royal Meteorological Society*, **143**, 2260-2271.

Yang, J., H. Chen, Y. Song, S. Zhu, B. Zhou, and J. Zhang, 2021: Atmospheric circumglobal teleconnection triggered by spring land thermal anomalies over West Asia and its possible impacts on early summer climate over northern China. *Journal of Climate*, **34**, 5999-6021.

Yeh T., S. Dao, and M. Li, 1958: The abrupt change of circulation over Northern Hemisphere during June and October. *Acta Meteor. Sinica*, **29**(4), 249-263. (in Chinese)

Zhou, W., L. R. Leung, and J. Lu, 2022a: Seasonally dependent future changes in the U.S. midwest hydroclimate and extremes. *Journal of Climate*, **35**, 17-27.

Zhou, T., and Coauthors, 2022b: 2021: A year of unprecedented climate extremes in Eastern Asia, North America, and Europe. *Advances in Atmospheric Sciences*, **39**, 1598−1607.